

RPE Damage Thresholds and Mechanisms for Laser Exposure in the Microsecond-to-Millisecond Time Regimen

Georg Schuele, Marco Rumohr, Gereon Huettmann, and Ralf Brinkmann

PURPOSE. The retinal pigment epithelium (RPE) cells with their strongly absorbant melanosomes form the highest light-absorbing layer of the retina. It is well known that laser-induced retinal damage is caused by thermal denaturation at pulse durations longer than milliseconds and by microbubble formation around the melanosomes at pulses shorter than microseconds. The purpose of this work was to determine the pulse width when both effects merge. Therefore, the RPE damage threshold and mechanism of the damage at single laser pulses of 5- μ s to 3-ms duration were investigated.

METHODS. An argon laser beam (λ 514 nm) was externally switched by an acousto-optic modulator to achieve pulses with constant power in the time range of 5 μ s up to 3 ms. The pulses were applied to freshly prepared porcine RPE samples serving as a model system. After laser exposure RPE cell damage was proved by the cell-viability stain calceinAM. Microbubble formation was detected by acoustic techniques and by reflectometry.

RESULTS. At a pulse duration of 5 μ s, RPE cell damage was always associated with microbubble formation. At pulses of 50 μ s, mostly thermal denaturation, but also microbubble formation, was detected. At the longer laser pulses (500 μ s, 3 ms), RPE cell damage occurred without any microbubble appearance.

CONCLUSIONS. At threshold irradiance, the transition time from thermal denaturation to thermomechanical damage of RPE cells is slightly below the laser pulse duration of 50 μ s. (*Invest Ophthalmol Vis Sci.* 2005;46:714-719) DOI:10.1167/iovs.04-0136

The interaction of laser radiation with biological tissue is of interest both for medical applications and for the establishment of laser safety standards. Laser treatments of retinal diseases are widely used in ophthalmology. Laser therapies at the fundus range from established continuous wave (cw) photocoagulation¹ to new ophthalmic laser applications, such as selective retinal pigment epithelium (RPE) treatment (SRT),² photodynamic therapy (PDT),³ and transpupillary thermotherapy (TTT).⁴ Maximum permissible exposure limits were established for visible and near-IR laser radiation from cw down to femtosecond exposures.⁵ The type of damage mechanism depends on the duration of the applied laser pulse. At cw to

10-ms exposure time, a pure thermal denaturation of tissue has been shown to be the primary retinal damage mechanism.⁶⁻⁹ In this time frame, the damage can be described as a damage integral based on the Arrhenius law.^{10,11} From microsecond to nanosecond exposure times, there is evidence that RPE damage is induced by intracellular microbubble formation around the strongly absorbant melanosomes inside the RPE cell.¹²⁻¹⁵ The microbubble formation leads to a disintegration of the RPE cell structure and a disruption of the cell membrane. At subnanosecond exposures, other nonlinear damage mechanisms appear, such as shock-waves and laser-induced breakdown.¹⁴

The RPE is the layer that absorbs the highest amount of light in the retina.^{6,16} The ellipsoidal shaped, approximately 1- μ m-sized melanosomes within these cells are the strongest chromophore for visible light of the fundus.¹⁷ In humans, approximately 60% of the incident light that reaches the retina is absorbed within this cell layer.¹⁸

Until now, the exact exposure time at which a change of damage mechanism from a pure thermal denaturation to thermomechanical damage occurs is unknown. In ANSI-Standard Z-136.1-2000⁵—the maximum allowed exposure—the change of damage mechanism has been defined as occurring at 18 μ s.⁵ Looking on a plot of the experimental damage threshold data over exposure time from ANSI-Standard Z-136.1-1993¹⁹ (also shown by Cain et al.²⁰), the change of slope at \sim 50 μ s of exposure time can be associated with a change in the damage mechanism. It has been shown that, below this exposure time, the laser-induced retinal temperature increase is limited mostly to the RPE cell layer.^{9,21} The thermal confinement increases the probability that temperatures will be induced that are above the vaporization threshold, which results in microbubble formation.

Acoustic measurements have been used to detect cavitation in water²² and to monitor laser-induced microbubble formation in RPE.²³⁻²⁶ During irradiation with a train of microsecond laser pulses, acoustic transients correlated with the damage of a few RPE cells.²⁴⁻²⁶ In similar experiments, the back-reflected light increase due to the formation of a bubble-water interface was used to confirm the formation of microbubbles in RPE during nano- and microsecond laser pulses.¹⁵

The purpose of this in vitro study was to determine the laser-induced RPE damage mechanism and damage thresholds by using acoustic and reflection measurements as well as cell-viability stains for pulse duration between 5 μ s and 3 ms.

METHODS

Setup

A sketch of the experimental setup is shown in Figure 1. A cw argon laser beam (514 nm; model 2030-15s; Spectra Physics, Mountain View, CA) was externally switched by an acousto-optic modulator (AOM) to achieve temporal rectangular pulse shapes of 5-, 50-, or 500- μ s or 3-ms width. The light was coupled to a 50- μ m diameter fiber (50- μ m core, numerical aperture [NA] 0.1; Coherent, Palo Alto, CA). The fiber tip was imaged with an ophthalmic slit lamp (Visulas; Carl Zeiss Meditec, Jena, Germany) on the RPE surface with a 50- μ m spot diameter on the

From the Medical Laser Center Lübeck, Lübeck, Germany.
Supported by Bundesministerium für Bildung und Forschung (BMBF) Grant 13N7309.

Submitted for publication February 10, 2004; revised August 17, 2004; accepted September 13, 2004.

Disclosure: **G. Schuele**, None; **M. Rumohr**, None; **G. Huettmann**, None; **R. Brinkmann**, None

The publication costs of this article were defrayed in part by page charge payment. This article must therefore be marked "advertisement" in accordance with 18 U.S.C. §1734 solely to indicate this fact.

Corresponding author: Georg Schuele, Department of Ophthalmology and W.W. Hansen Experimental Physics Laboratory, Stanford University, 445 Via Paolo, Stanford, CA 94305-4085; schuele@stanford.edu.

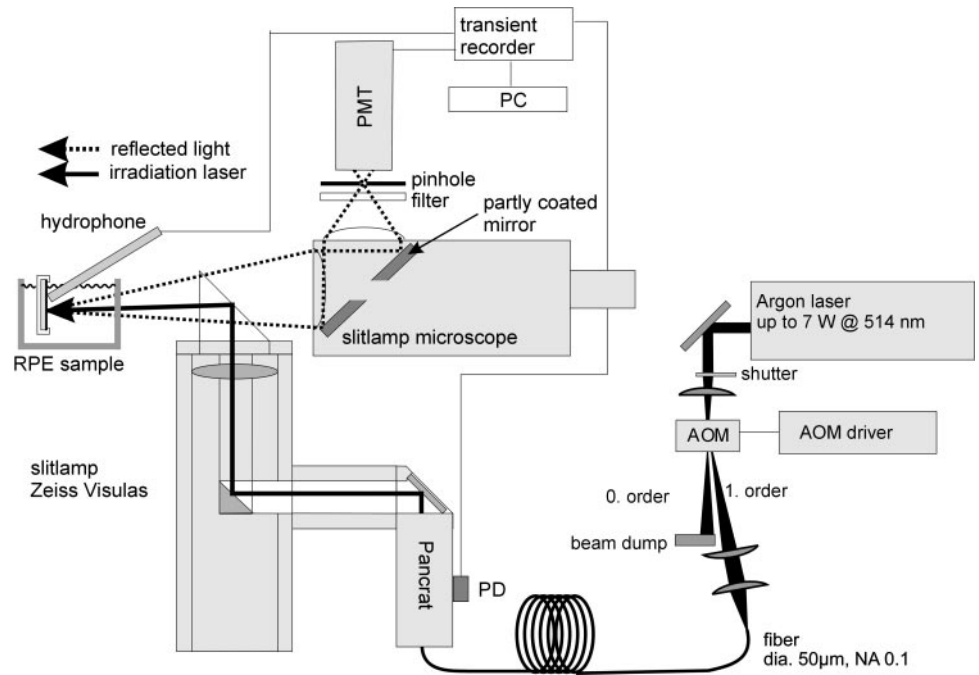


FIGURE 1. Experimental irradiation setup.

sample. The spatial beam profile was a circular tophat, which was modulated by speckle formation. The beam profile in the sample plane was measured 20 times with a beam analyser (model LBA-300PC; Spiricon Inc., Logan, UT). The average size of the speckle was $4 \mu\text{m}$ and the maximum radiant exposure was 3.80 ± 0.03 (SD) higher than the average. Two physically independent methods were used to detect microbubble formation during exposure. First, the acoustic emission during microbubble formation was detected with a hydrophone (VP-1093, 0–10 MHz, 1.05 V/bar; Valpey-Fisher, Hopkinton, MA; preamplified with model 5676, 40 dB, 50 kHz–20 MHz; Panametrics, Waltham, MA). Second, the increased light reflection from the sample due to the generated bubble-water interface was confocally imaged to a photomultiplier (Typ R1436; Hamamatsu, Hamamatsu City, Japan). All data were recorded by a transient recorder (model RTD710; Sony/Tek, Tokyo, Japan) and transferred to a computer (LabView, ver. 6i; National Instruments, Austin, TX).

Sample Preparation and Vitality Staining

As RPE samples, freshly enucleated porcine eyes from an abattoir were used. After an equatorial opening of the eye globe, the vitreous body was removed, and a 1-cm²-sized sample was prepared. The neural retina including the photoreceptor layer was gently peeled off. The sample with the vital RPE cells in a superficial layer was covered with phosphate-buffered saline (PBS) and fixed in the sample holder. The samples were irradiated with single pulses of 5- μs ($\Sigma = 480$ spots), 50- μs ($\Sigma = 270$ spots), 500- μs ($\Sigma = 192$ spots), or 3-ms ($\Sigma = 546$ spots) duration. All laser pulse durations were investigated in at least 10 samples of 10 different eyes. After irradiation, the sample was stained with the cell viability marker calceinAM (Molecular Probes, Eugene, OR). Because of the uncharged structure of calceinAM, it can penetrate the cell membrane. Once inside the cell, the lipophilic blocking groups are cleaved by nonspecific esterases. This intracellular released calcein fluoresces when excited with 480-nm light. Living cells fluoresce brightly because of the accumulated calcein, whereas cells without esterases appear dark in the fluorescence microscope image. Figure 2 shows a typical fluorescence microscopic image of a sample with damaged cells after exposure.

Data Analysis

For analysis of the measured acoustic transients $P(t)$ the acoustic energy E_A was calculated by:

$$E_A = \int_0^{\pi} (P(t))^2 dt$$

An acoustic energy threshold for microbubble formation could be defined, and the acoustic energy values were sorted in dichotomous values (1 $\hat{=}$ acoustically detected microbubble formation; 0 $\hat{=}$ no microbubble).

From the viability-stained fluorescence microscopic images of the RPE samples, cell viability was sorted in dichotomous values (1 $\hat{=}$ vital cell, 0 $\hat{=}$ dead cell).

All thresholds of RPE damage and bubble formation were examined by Probit analysis^{27,28} on a logarithmic dose scale (SPSS, 7.0; SPSS, Chicago, IL). In general, the ED_{84} and the corresponding ED_{16} describe the width of the adjusted normal distribution with logarithmic covariant basis.²⁸ The software would calculate only ED_{85} and ED_{15} instead of the specified ED_{84} and ED_{16} , but the deviations are negligible.

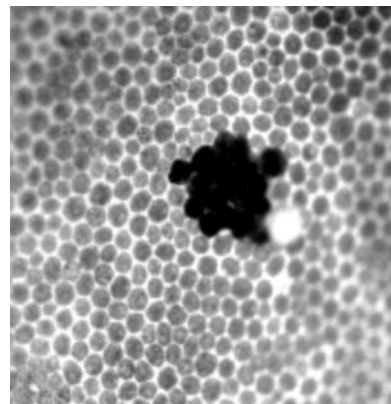


FIGURE 2. Porcine RPE cells stained with calceinAM. Live cells fluoresce, and dead cells appear dark.

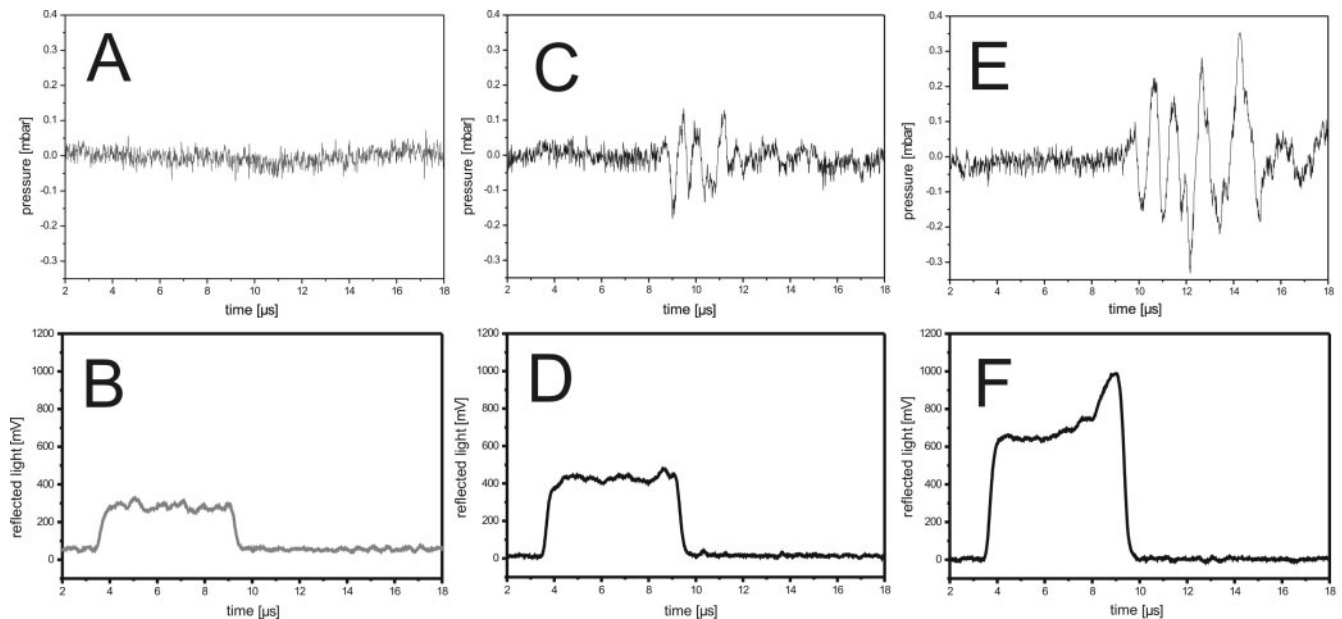


FIGURE 3. Acoustic transients (A, C, E) and the associated measured reflected light signals (B, D, F) during irradiation of porcine RPE samples with single 5- μ s laser pulses: (A-D) 256 mJ/cm²; (E, F) 440 mJ/cm².

RESULTS

To give an overview of the experimental results, some typical measured signals are shown for the shortest (5- μ s) and the longest (3-ms) pulse duration.

Measured Acoustic Transients and Reflectance Signals for the 5- μ s Pulse Duration

For the 5- μ s pulse duration, three acoustic transients and the reflected light signals are shown in Figure 3. At a low-radiance exposure of 256 mJ/cm², which did not damage the RPE, no acoustic transient above the noise level of 50 μ bar could be measured (Fig. 3A). Acoustic transients due to thermoelastic expansion were too weak to detect. In the reflected light signal, only the diffuse reflected laser pulse time course could be measured (Fig. 3B). If no acoustic transients were measured, all cells were viable after the exposure.

At the same energy and in the same RPE sample but at a different location, an increased acoustic transient was measured (Fig. 3C), indicating microbubble formation. Although, no significant increase of the reflected laser pulse form was detectable (Fig. 3D), no RPE cells were damaged. This effect of an acoustically detectable microbubble formation without RPE damage was measured 12 times in the 480 applied 5- μ s laser pulses.

At higher radiance exposure (440 mJ/cm²) the acoustic transient amplitude (Fig. 3E) increased compared with that in Figure 3C. With this exposure, 100% of the illuminated RPE cells were damaged. Close to the end of the laser pulse, the reflected light signal increased significantly (Fig. 3F). This effect was most likely induced by microbubble formation, as the RPE temperature was highest at the end of the laser pulse.

At all applied radiance exposures, the analyzed acoustic energy correlated with the percentage of RPE cell damage in the irradiated area. Figure 4 shows the acoustic energy over the percentage of damaged RPE cells for one sample. In this plot, there are typically three different areas of interest: (1) region A, without damaged RPE cells; only the acoustic energy of the secondary background noise, such as the electric noise of the amplifier (as shown in the acoustic transient Fig. 3A), was

detected; (2) region B, without damaged RPE cells, but increased acoustic energy indicated microbubble formation (as shown in the acoustic transient Fig. 3C); and (3) region C with at least a certain fraction of damaged RPE cells; the acoustic energy was strongly increased, indicating the formation of microbubbles (as shown in the acoustic transient Fig. 3E). These three kinds of areas appeared in all 10 irradiated RPE samples.

An acoustic energy threshold value for microbubble formation can be defined. After Probit analysis of the data from the 10 RPE samples, the thresholds for microbubble formation were $ED_{50}^{acoust} = 223$ mJ/cm² ($ED_{15}^{acoust} = 168$ mJ/cm²; $ED_{85}^{acoust} = 277$ mJ/cm², slope = 8.4) and for RPE damage

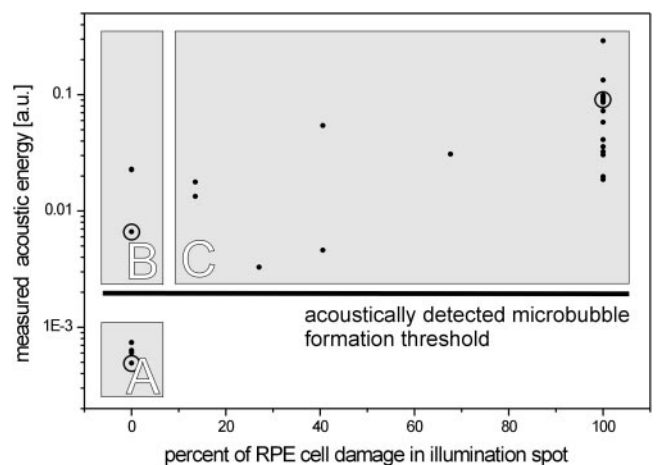


FIGURE 4. Measured acoustic energy of the acoustic transients for 5- μ s pulse duration over the percentage of damaged RPE cells within the illumination spot. *Black, circled data points* correspond to the data in Figure 3. A threshold for acoustically detectable microbubble formation can be defined. Three areas of interest are marked: A, no RPE damage, low acoustic energy only from secondary background noise; B, no RPE damage, but acoustic transients with acoustic energy above the noise level; C, various percentages of RPE damage within the illumination spot, acoustic energy above the noise level.

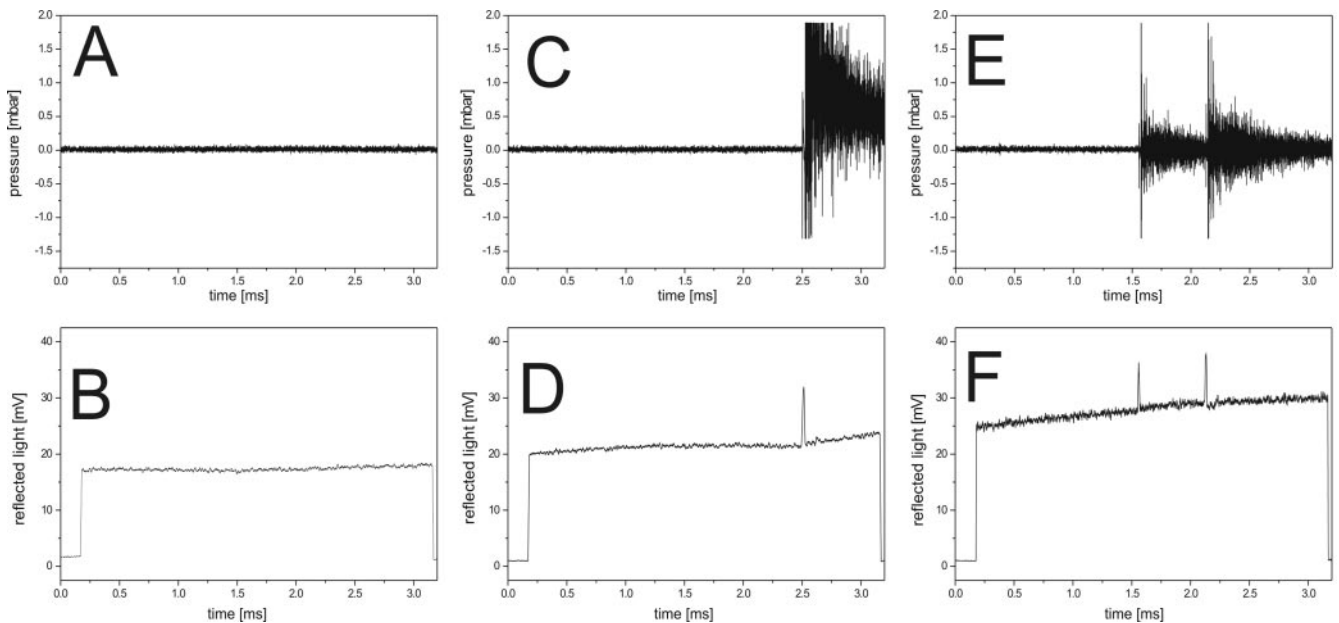


FIGURE 5. Acoustic transients (A, C, E) and the associated measured reflected light signals (B, D, F) during irradiation of porcine RPE samples with single 3-ms laser pulses: (A, B) 8.4 J/cm²; (C, D) 12 J/cm²; (E, F) 16 J/cm².

were $ED_{50}^{\text{damage}} = 252 \text{ mJ/cm}^2$ ($ED_{15}^{\text{damage}} = 166 \text{ mJ/cm}^2$; $ED_{85}^{\text{damage}} = 359 \text{ mJ/cm}^2$, slope = 8.2). The relatively large difference between ED_{15} and ED_{85} is due to the variations of the RPE damage threshold in the different RPE samples.

Measured Acoustic Transients and Reflectance Signals for 3-ms Pulse Duration

At the 3-ms pulse duration, three acoustic transients and the attendant reflected light signals are shown in Figure 5. In all cases, 100% of the RPE cells within the spot were damaged. No acoustic transient from microbubble formation was detected in spots where <100% of irradiated cells were damaged.

At a radiance exposure of 8.6 J/cm², no acoustic transient (Fig. 5A) and no significant increase of reflected light (Fig. 5B) was detected. Raising the exposure to 12.7 J/cm² resulted in microbubble formation, which was detected as well by the acoustic transient (Fig. 5C) as by a reflected light signal peak (Fig. 5D). The temporal onset of both signals correspond exactly, if the acoustic transit time from the sample to the transducer is taken into account. The measured acoustic pressure amplitude was 25 times higher than in the 5- μs experiments. Low-pressure amplitudes, as detected during the 5- μs exposures were never found with 3-ms laser pulses. The lifetime of the generated bubble was determined from the reflected light signal peak as 20 μs . Multiple oscillating microbubble bursts were generated by increasing the radiance exposure to 17.3 J/cm² (Figs. 5E, 5F).

For this RPE sample, the analyzed acoustic energy values were plotted over the percentage of RPE cell damage (Fig. 6). They can be grouped into two areas of interest: region A, with various percentages of RPE damage, but no microbubble formation; and region B, with only 100% damaged cells and microbubble formation.

Also, in this case, a threshold value for microbubble formation can be defined. Probit analysis of the data from all 10 RPE samples showed that the threshold of microbubble formation of $ED_{50}^{\text{acoust}} = 12.1 \text{ J/cm}^2$ ($ED_{15}^{\text{acoust}} = 9.4 \text{ J/cm}^2$, $ED_{85}^{\text{acoust}} = 14.8 \text{ J/cm}^2$, slope = 9.4) was nearly three times the RPE damage threshold of $ED_{50}^{\text{damage}} = 4.3 \text{ J/cm}^2$ ($ED_{15}^{\text{damage}} = 3.5 \text{ J/cm}^2$, $ED_{85}^{\text{damage}} = 5.4 \text{ J/cm}^2$, slope = 10.2).

Damage Thresholds and Mechanisms

Exposure thresholds for RPE damage and microbubble formation at different pulse durations are shown in Figure 7 and summarized in Table 1. The error bars correspond to the ED_{15} and ED_{85} of the Probit analysis. At a 5- μs laser pulse duration, the RPE damage threshold was slightly above the threshold for microbubble formation. This changed at 50- μs laser pulses, which resulted in a damage threshold slightly below the threshold for microbubble formation. At the longer pulse durations of 500 μs and 3 ms, the threshold for microbubble formation was nearly two and three times more than the RPE damage threshold, respectively. Each single RPE sample showed a very sharp and significant damage threshold. The relatively wide distribu-

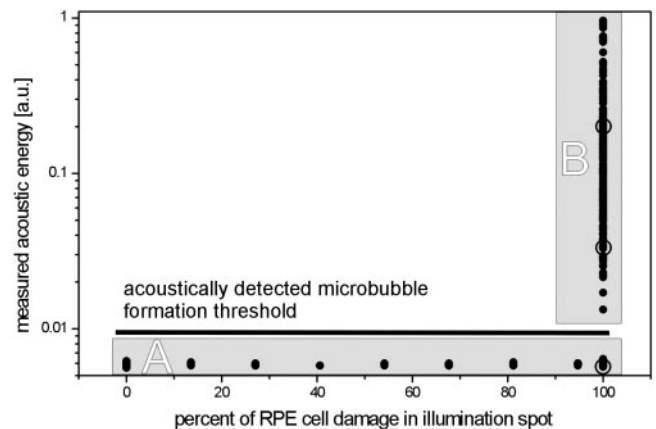


FIGURE 6. Measured energy of the acoustic transients at a 3-ms pulse duration over the percentage of damaged RPE cells within the illumination spot. Black circled data points correspond to the data in Figure 5. A threshold value for acoustically detectable microbubble formation can be defined. Two areas of interest are marked: A, up to 100% RPE damage within the spot but low acoustic energy signals, indicating no microbubble formation; B, only 100% RPE damage and high acoustic energy values indicating microbubble formation starting at radiant exposures nearly three times over the RPE damage threshold.

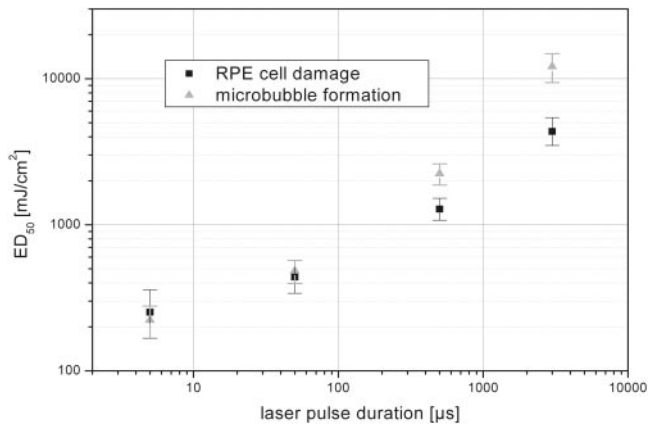


FIGURE 7. RPE damage and microbubble formation threshold (ED_{50}) for single laser pulses from 5- μ s to 3-ms laser pulse duration. The error bars correspond to the ED_{15} and ED_{85} values of the logarithmic normal distribution, which was adjusted by the Probit algorithm.

tion between ED_{15} and ED_{85} is due to the variation of the sample-specific thresholds.

For determining the primary damage mechanism, the correlation of cell death with bubble formation was calculated for the different laser pulse durations. Only experiments in the RPE damage threshold region ED_{10} to ED_{90} were included. By limiting the analysis to the threshold region ED_{10} to ED_{90} , only the primary damage mechanism in the region slightly wider than the width of the normal distribution with logarithmic covariant basis was evaluated. Effects such as bubble formation at threefold ED_{50} exposure as seen with 3-ms laser pulses in Figures 5E and 5F were excluded. At all laser pulse durations, the results were sorted into the frequency of RPE damage, with and without acoustically detectable microbubble formation (Fig. 8). This classification shows, that if RPE cells are damaged, microbubble formation can always be detected with a 5- μ s laser pulse duration. At a 50- μ s laser pulse duration, only 16% of the RPE cells were damaged combined with microbubble formation. At 500- μ s and 3-ms pulses, the RPE cells were damaged without microbubble formation in the threshold range of ED_{10} to ED_{90} .

DISCUSSION

Detection of Microbubble Formation

It has been shown by Rögner et al.¹⁵ that the detection of intracellular microbubble formation during laser irradiation of RPE samples is possible by monitoring the back-reflected light. We used two physically independent methods for the detection of microbubble formation during laser exposure of the RPE. The simultaneous detection of microbubble formation by an increase in reflected light signal and also an increase of the

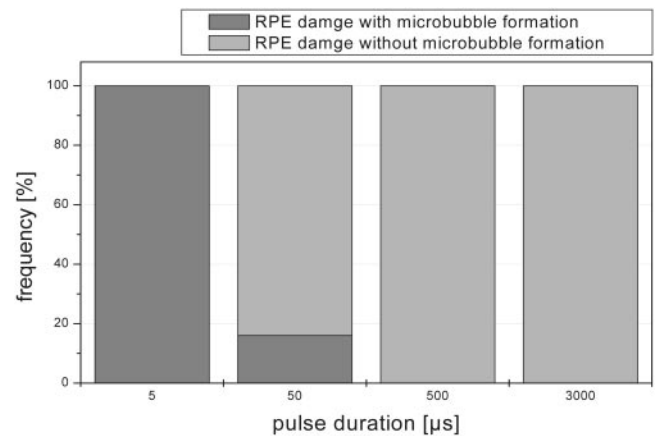


FIGURE 8. Frequency of RPE damage with or without acoustically detectable microbubble formation at laser pulse durations in the threshold region ED_{10} to ED_{90} .

acoustic transient clearly indicates microbubble formation (Figs. 3E, 3F). In our experiments, the acoustic detection was more sensitive than the reflected light signal. Microbubble formation was clearly detected by the onset of an acoustic transient without detectable change in the reflected light (Figs. 3C, 3D). Although the reflected-light detection method was less sensitive, it provided additional information over the bubble's lifetime, as seen in Figures 4C-F. At the short pulse durations of 5 μ s, it was not possible to determine the bubble's lifetime reliably, due to the limited irradiation time.

RPE Damage Thresholds

The measured porcine RPE damage threshold of $ED_{50}^{\text{damage}} = 252 \text{ mJ/cm}^2$ for single 5- μ s laser pulses are in good agreement with data of single 3- μ s laser pulses of 232 mJ/cm^2 at 527 nm of Rögner et al.^{9,21} In a more recent study they reported a damage threshold of 412 mJ/cm^2 at 532 nm for single 6- μ s laser pulses¹⁵ in a similar experimental system. At all other pulse durations, no RPE or retinal damage exposure thresholds are accessible.

RPE Damage Mechanism

In our study, at a 5- μ s laser pulse duration, RPE damage always coincided with the formation of microbubbles. It is remarkable that in some cases microbubble formation was detected without RPE cell damage at the 5- μ s laser pulse duration (Figs. 3C, 3D). Therefore RPE cells were able to survive the formation of small or few microbubbles. It can be assumed, that this caused a volume increase too small to disrupt the cellular membranes. These rare cases with microbubble formations without cell damage lead to a threshold of microbubble formation below the RPE damage threshold. This is in contrast to the results of

TABLE 1. RPE Cell Damage and Microbubble Formation Threshold Data, Confidence Intervals and Probit Slopes from Figure 7

Laser Pulse Duration	Number of Applied Laser Pulses	RPE Cell Damage				Microbubble Formation			
		ED_{50}	ED_{15}	ED_{85}	Probit Slope	ED_{50}	ED_{15}	ED_{85}	Probit Slope
5 μ s	480	252	166	359	8.2	222	168	277	8.4
50 μ s	270	439	340	567	9.4	483	396	570	12
500 μ s	192	1278	1075	1519	13.8	2242	1871	2613	13.2
3ms	546	4346	3488	5414	10.2	12106	9397	14815	9.4

ED data are in microjoules per square centimeter.

Rögener et al.¹⁵ with single 6- μ s laser pulses. It appears that their reflected light-based detection setup was not sensitive enough to monitor small microbubbles in a manner similar to our setup.

In a recent study,²⁹ we also demonstrated that the acoustic detection of microbubble formation during patient treatment with a train of 1.7- μ s laser pulses for the selective treatment of the RPE (SRT)² coincides with the angiographic retinal leakage of fluorescein after treatment. Angiographic leakage in the retina indicates damaged RPE cells or at least damaged tight junctions between the RPE cells, which act as the blood-retina barrier. Because the induced angiographic lesions on the patients retina were ophthalmoscopically invisible, and the overlying photoreceptors in the treated spot were still functioning,³⁰ microbubble formation seems to be the primary damage mechanism of the retina in humans at this pulse duration.

At the 50- μ s laser pulse duration, our data show that the death of RPE cells without microbubble formation was dominant (Fig. 8). However, damage with microbubble formation was observed in 16% of the irradiated spots with radiant exposure in the range of ED₁₀ to ED₉₀.

At the longer laser pulse durations of 500 μ s and 3 ms, all cell death occurred without bubble formation (Fig. 8). This is in good correspondence with the data from other studies.⁶⁻⁹ At these pulse durations, microbubble formation occurred at the twofold (500 μ s) to threefold (3 ms) RPE damage threshold and can be clearly stated not to be the primary mechanism of RPE damage.

Our results show that both damage mechanisms merge at laser pulse durations only slightly shorter than 50 μ s. This result is in good agreement with the change of damage threshold slope of the ANSI-Standard Z-136.1-1993¹⁹ (also shown by Cain et al.²⁰) at ~50- μ s laser pulse duration, which can be associated with a change of damage mechanism.

CONCLUSION

Acoustic measurements allow a detailed insight into laser-induced RPE damage mechanisms. This technique is extremely sensitive and even allows the detection of microbubble formation inside the RPE cell if no RPE damage occurs.

At a 5- μ s laser pulse duration, microbubble formation has been shown to be the primary RPE damage mechanism. The point of change from thermomechanical microbubble-induced RPE cell damage to pure thermal RPE denaturation is ~50- μ s exposure time. At longer pulse durations, the primary damage mechanism is purely thermal.

References

1. Macular Photocoagulation Study Group. Laser photocoagulation of subfoveal recurrent neovascular lesions in age-related macular degeneration: results of a randomized clinical trial. *Arch Ophthalmol.* 1991;109:1232-1241.
2. Roeder J, Brinkmann R, Wirbelauer C, et al. Subthreshold (retinal pigment epithelium) photocoagulation in macular diseases: a pilot study. *Br J Ophthalmol.* 2000;84:40-47.
3. Treatment of Age-Related Macular Degeneration with Photodynamic Therapy (TAP) Study Group. Photodynamic therapy of subfoveal choroidal neovascularization in age-related macular degeneration with verteporfin: one-year results of 2 randomized clinical trials—TAP report. *Arch Ophthalmol.* 1999;117:1329-1345.
4. Reichel E, Berrocal AM, Ip M, et al. Transpupillary thermotherapy of occult subfoveal choroidal neovascularization in patients with age-related macular degeneration. *Ophthalmology.* 1999;106:1908-1914.
5. ANSI. *Safe Use of Lasers.* Orlando, FL: American National Standards Institute; 2000:Z-136.1-2000.

6. Birngruber R, Hillenkamp F, Gabel V-P. Theoretical investigations of laser thermal retinal injury. *Health Phys.* 1985;48:781-796.
7. Birngruber R. Thermal modelling in biological tissue. In: Hillenkamp F, ed. *Lasers in Biology and Medicine.* New York: Plenum Publishing; 1980:77-97.
8. Birngruber R. Choroidal circulation and heat convection at the fundus of the eye. In: Wolbarsht ML, ed. *Laser Applications in Medicine and Biology.* Vol. 5. New York: Plenum Publishing; 1991:277-361.
9. Sliney DH, Marshall J. Tissue specific damage to the retinal pigment epithelium: mechanisms and therapeutic implications. *Lasers Light Ophthalmol.* 1992;5:17-28.
10. Birngruber R, Gabel V-P, Hillenkamp F. Experimental studies of laser thermal retinal injury. *Health Phys.* 1983;44:519-531.
11. Birngruber R, Hillenkamp F, Gabel V-P. *Experimentelle und theoretische Untersuchungen zur thermischen Schädigung des Augenhintergrundes durch Laserstrahlung.* München: Gesellschaft für Strahlen-und Umweltforschung MBH München; 1978.
12. Brinkmann R, Huettmann G, Rogener J, et al. Origin of retinal pigment epithelium cell damage by pulsed laser irradiance in the nanosecond to microsecond time regimen. *Lasers Surg Med.* 2000;27:451-464.
13. Lin CP, Kelly MW. Cavitation and emission around laser-heated microparticles. *Appl Phys Lett.* 1998;72:1-3.
14. Kelly MW. *Intracellular Cavitation as a Mechanism of Short-Pulse Laser Injury to the Retinal Pigment Epithelium.* Thesis. Medford, MA: Tufts University; 1997.
15. Roeger J, Brinkmann R, Lin CP. Pump-probe detection of laser-induced microbubble formation in retinal pigment epithelium cells. *J Biomed Opt.* 2004;9:367-371.
16. Gabel V-P, Birngruber R, Hillenkamp F. Die Lichtabsorption am Augenhintergrund: gesellschaft für Strahlen-und Umweltforschung. 1976;GSF-Bericht A55.
17. Schrämeyer U, Heimann K. Current understanding on the role of retinal pigment epithelium and its pigmentation. *Pigment Cell Res.* 1999;12:219-236.
18. Hammond BR, Caruso-Avery M. Macular pigment optical density in a southwestern sample. *Invest Ophthalmol Vis Sci.* 2000;41:1492-1497.
19. ANSI. *Safe Use of Lasers.* Orlando, FL: American National Standards Institute; 1993:Z-136.1-1993.
20. Cain CP, Toth CA, Noojin GD, et al. Thresholds for visible lesions in the primate eye produced by ultrashort near-infrared laser pulses. *Invest Ophthalmol Vis Sci.* 1999;40:2343-2349.
21. Rögener J. *Schadensmechanismus bei der Laserbestrahlung des retinalen Pigmentepithels mit Nano- und Mikrosekundenpulsen.* Medizinisches Laserzentrum Lübeck. Thesis. Lübeck, Germany: Universität Hamburg, 1998.
22. Vogel A, Lauterborn W. Acoustic transient generation by laser-produced cavitation bubbles near solid boundaries. *J Acoust Soc Am.* 1988;84:719-731.
23. Schuele G, Huettmann G, Roeder J, et al. Optoacoustic measurements during μ s-irradiation of the retinal pigment epithelium. *Proc SPIE.* 2000;3914:230-236.
24. Schuele G, Joachimmeyer E, Framme C, et al. Optoacoustic detection of selective RPE cell damage during μ s laser irradiation. *Proc SPIE* 2001;4433:92-96.
25. Schuele G, Joachimmeyer E, Framme C, et al. Optoacoustic control system for selective treatment of the retinal pigment epithelium. *Proc SPIE* 2001;4256:71-76.
26. Schuele G. *Mechanisms and Online Dosimetry for Selective RPE Treatment* (in German). Medical Laser Center Lübeck. Lübeck, Germany: University of Lübeck, 2003.
27. SPSS. *Technical Support: Probit.* ver. 5.0. Chicago, IL: SPSS; 2001.
28. Sliney DH, Mellerio J, Gabel V-P, Schulmeister K. What is the meaning of threshold in laser injury experiments?—implications for human exposure limits. *Health Phys.* 2002;82:335-347.
29. Schuele G, Elsner H, Hoerauf H, et al. Optoacoustic online dosimetry during selective RPE treatment. *Proc SPIE.* 2004;5314:286-297.
30. Roeder J, Hillenkamp F, Flotte T, Birngruber R. Microphotocoagulation: selective effects of repetitive short laser pulses. *Proc Natl Acad Sci.* 1993;90:8643-8647.